Experimental and computational investigation of tensile and flexural properties of polylactic acid filled with boron nitride nanoplatelets

Harishbabu Sundarasetty, Santosh Kumar Sahu*
School of Mechanical Engineering, VIT-AP University, Besides A.P. Secretariat, Amaravati 522237, Andhra Pradesh, India
harish.24phd7063@vitap.ac.in, https://orcid.org/0000-0001-9317-4963
sksahumech@gmail.com, http://orcid.org/0000-0002-6729-0415

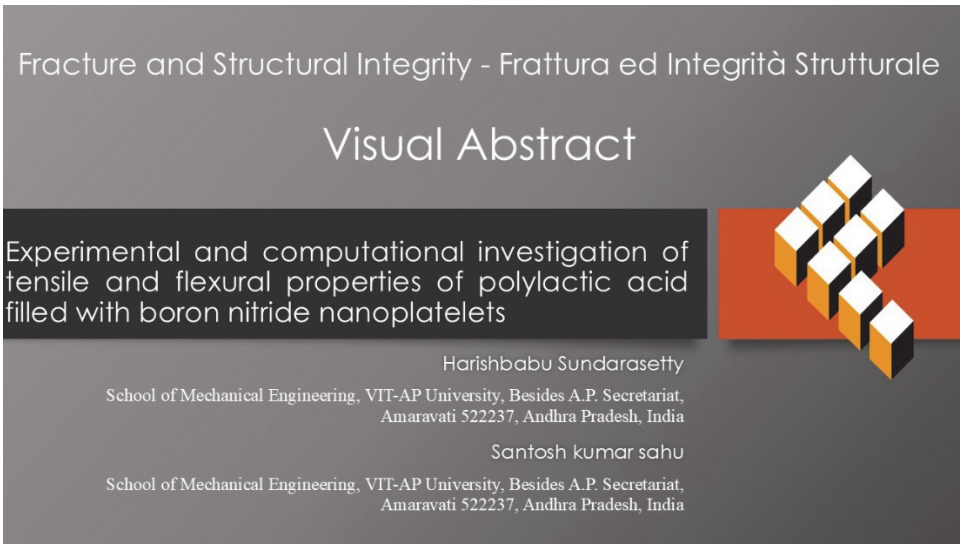

Citation: Sundarasetty, H., Sahu, S. K., Experimental and computational investigation of tensile and flexural properties of polylactic acid filled with boron nitride nanoplatelets, Fracture and Structural Integrity, 72 (2025) 211-224.

Received: 14.02.2025
Accepted: 17.03.2025
Published: 19.03.2025
Issue: 04.2025

Copyright: © 2025 This is an open access article under the terms of the CC-BY 4.0, which permits unrestricted use, distribution, and reproduction in any medium, provided the original author and source are credited.

KEYWORDS. Micromechanical model, Polylactic acid (PLA), Boron Nitride Nanoplatelets (BNNP), Finite Element Analysis (FEA).

INTRODUCTION

Polylactic acid (PLA), commonly referred to as polylactide, is an eco-friendly, renewable and biodegradable thermoplastic polyester sourced from sustainable materials like corn, sugarcane, cassava or the pulp of sugar beets [1], unlike traditional polymers being non-degradable that are typically derived from fossil fuels and petroleum-based origins. PLA demonstrates bio-friendly and facile decomposition and is regarded as a green material. It maintains impressive strength and rigidity at room temperature. PLA is utilized in numerous sectors, such as food packaging, electronics, automotive and medical apparatus. Introducing nanoparticles into the PLA matrices can improve their mechanical properties, making them more suitable for green composites. The following describes the results of a few important literature papers in the area of concern related to our research.

According to research by Ajaj et al. [2], adding graphene nanoparticles (Gr) (0 to 0.5 wt. %) increased the yield stress and elongation at an optimum concentration of 0.4 wt.% PLA/Gr. The addition of further filler in the PLA matrix showed a decreasing trend due to particle agglomeration. Nethula et al. [3] reported that the incorporation of 2 wt. % of sulphur-doped titanium dioxides (S-TiO_2) into the polylactic acid (PLA) enhanced hardness, flexural strength and tensile strength by 10.3%, 23.2% and 20%, respectively. *The research by Thangarajan et al. [4] demonstrated* that the incorporation of recovered carbon black (RCB) with varying mesh sizes (500, 1000,1500 and 2000) significantly enhanced the tensile strength of polylactic acid (PLA), elevating it from 28.6 MPa to 47.2 MPa. Additionally, the elastic modulus increased from 832 MPa to 1.56 GPa. According to Petousis et al. [5], Zirconium Dioxide (ZrO_2) loading between 1 and 3 wt. % in PLA and polyamide 12 (PA12) caused an increase in tensile strength of 20.1% for PLA at 1 wt. %, while PA12 at a 3 wt.% filler content yields a 47.7%. Li et.al [6] investigation revealed that Graphene-reinforced polylactic acid (G-PLA) nanocomposites exhibited significantly improved mechanical characteristics, demonstrating a 182% augmentation in Young's modulus alongside an 85% enhancement in tensile strength. Makri et al. [7] showed that reinforcing PLA with 2.3 wt% nano lignin (NL) tripled its tensile strength, while PLA-L/NL achieved Young's modulus of 1380 MPa (5 wt% lignin) and 1373 MPa (2.5 wt% nano-lignin), compared to 638 ± 50 MPa for pure PLA. Huang et al. [8] analysed the mechanical properties of PLA reinforced with 0 to 3 wt. % carbon nanotubes (CNT). Their results showed an improved elongation at break, tensile strength, and Young's modulus value at the higher filler concentrations. According to a study by Solechan et al. [9], the PLA/polycaprolactone *(PCL)*/nano-hydroxyapatite *(*nHA) composite with 80%, 20% and 10% PLA, PCL and nHA demonstrated superior mechanical qualities of 55.35 MPa of flexural strength and 30.68 MPa of tensile strength. Khammassi et al. [10] studied the impacts of four different nanofillers on the mechanical characteristics of PLA composites. The Vermiculite (VMT) /hexadecyltrimethylammonium bromide (HDTMA)/PLA composite sample had superior and increased elastic modulus and stiffness respectively, compared to the pristine PLA. Vidakis et al. [11] showed adding 4 wt. % *tungsten carbide* (WC) in PLA improved the tensile strength by 42.5% and flexural strength by 41.9%. Dileep et al. [12] reported on PLA composites filled with equal weightage of graphene (*Gr) and* silicon dioxide (SiO_2) at 0.1 to 0.5 wt. %. Their results revealed that the optimum concentration was 0.3 wt. % of Gr and SiO_2, which increased the tensile and flexural strength compared to PLA from 29% to 60% and from 5% to 57% respectively. Sairy et al. [15] found that adding 3 wt. % graphene/nano clay to PLA nanocomposites resulted in a substantial enhancement of flexural strength and modulus, with 37% and 31% increases, respectively. He et al. [16] ascertained the *i*mpact of core-shell nanoparticles (silica core, poly (butyl acrylate) (PBA) shell) on the mechanical properties of PLA. Nanocomposites with 1 wt.% filler (SiO_2, SiO_2-NH_2, SiO_2-PBA-NH_2) showed a 17.6% increase in tensile strength for PLA/SiO_2-NH_2 and 36.9% for PLA/SiO_2-PBA-NH_2, compared to 4.2% for PLA/SiO_2. Additionally, core-shell nanoparticles improved the ductility, increasing the elongation at a break by 25.9%. Park et al. [17] noticed an increase in tensile strength and elongation at break by 38% and 42%, respectively, at 1 wt. % of PLA/Alkylated Graphene Oxide (AGO) in contrast to neat PLA. Campuzano et al. [18] investigated the influence of carbon dots (CDs) at a concentration varying from 0.1 to 5 wt. % on the mechanical properties of PLA composites. The optimum concentration was observed at 0.3 wt. % of CDs, where the tensile modulus and strength increased compared with pure PLA from 3.55 to 4.3 GPa and 30 to 55 MPa*,* respectively.

Extensive research has been conducted on PLA reinforced with various nanofillers, such as graphene (Gr), carbon nanotubes (CNT), amino-functionalized graphene oxide (AGO), clay, silicon dioxide (SiO_2) and carbon dots (CDs). However, to the best of the authors' knowledge, no studies have comprehensively addressed this specific topic. Traditional research methods have mainly focused on experimental approaches to assess the tensile and flexural strength of PLA nanocomposites. While these methods provide valuable insights, they often lack predictive capabilities. To overcome this limitation, the present study introduces a finite element (FE) based Representative Volume Element (RVE) model to estimate Young's modulus of the PLA/BNNP composites, representing a novel contribution to the field. Boron nitride nanoplatelets (BNNP) were selected as the nanofiller due to their superior mechanical properties. The primary objective of this research was to fabricate the PLA/BNNP nanocomposites and evaluate their tensile and flexural properties through experimental and FE simulations.

MATERIALS AND METHODS

Materials

PLA pallets with a density of 1.20 to 1.30 g/cc and a melt flow index (MFI) of g/10 min were supplied by Banka BioLoo Ltd., India. The Boron nitride nanoplatelets (BNNP), with an average particle size of less than 100 nm, were provided by Nano Research Elements, India and used as a nanofiller in the process of the polymer nanocomposite fabrication.

Scanning Electron Microscopy (SEM)

The samples were examined using scanning electron microscopy (SEM), with ZEISS EVO 10 High-Resolution SEM (Carl Zeiss AG, Germany) having 20 nm resolution and 1KV SE. The filler structure of the BNNP was confirmed as a platelet structure from SEM imaging, as shown in Fig. 1. The fractography study was also carried out using SEM imaging, which will be discussed in a subsequent section.

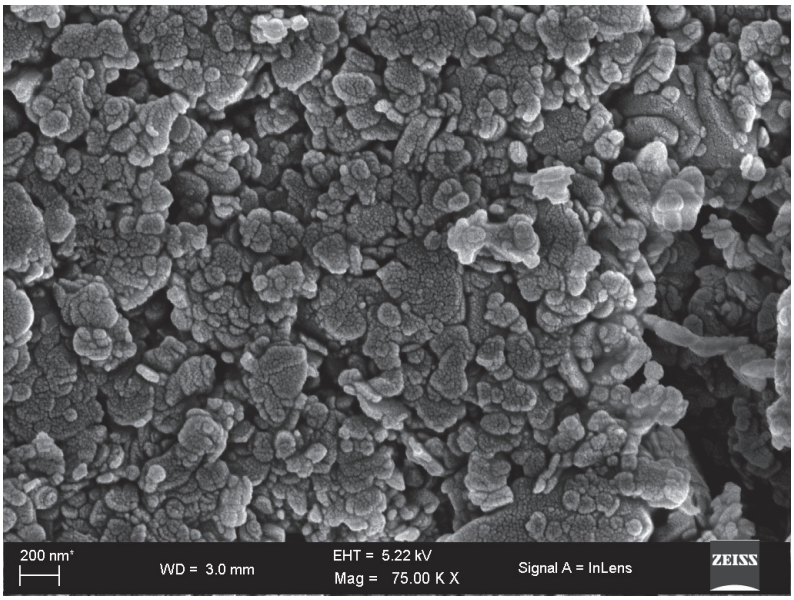

Figure 1: SEM image of received BNNP filler.

MICROMECHANICAL MATHEMATICAL MODELS

Mori-Tanaka model

The Mori-Tanaka approach is a helpful micromechanical method for evaluating the general modulus of composite materials. The interactions between the matrix and the inclusions are considered, resulting in accurate prediction. Eqn. (1) can be used for evaluating the composite modulus, it is a simplified version of the equation developed by Zhao et al. [19]

$$E_c = E_m \frac{\left(1+\frac{V_f}{1-V_f}\right)+3\left(\frac{1-V_f}{E_m+\left(\frac{1-V_f}{E_f}\right)}\right)}{\left(1+\frac{V_f}{1-V_f}\right)-3\left(\frac{1-V_f}{E_m+\left(\frac{1-V_f}{E_f}\right)}\right)} \quad (1)$$

E_c, E_m and E_f denote the moduli of the composite, matrix, and filler respectively. Additionally, V_f represents the volume fraction of filler material.

Self-Consistent model

The self-consistent method is a micromechanical approach used to evaluate the modulus of composite materials. It considers the interaction between the matrix and filler to provide a precise estimate of the moduli of the composites. Simplified by Kanaun et al. [20], Eqn. 2 may be referred-

$$E_c = E_m \left[1 + \frac{V_f \left(E_f - E_m \right)}{E_m + \left(\frac{1 - V_f}{3V_f} \right) E_f} \right] \quad (2)$$

The symbols adopted in Eqn. 2, are represented as E_c, E_m and E_f denotes moduli of composite, matrix, and filler respectively. V_f represents the volume fraction of filler material.

Fabrication of Composite samples

To fabricate the composite samples, the PLA matrix reinforced with BNNP filler was used at various weight percentages (wt%) 0.005, 0.01, 0.02, 0.03, and 0.04. The detailed steps adopted for the PLA/BNNP composite sample fabrication process are described in Fig. 2. The process used the melt mixing method to fabricate the PLA/BNNP composites, according to Jose et al. [18]. Initially, in a glass beaker, the weight of the BNNP filler was determined by a Weighing balance (Shimadzu ATX-224, Shimadzu Co., Japan) and then ethanol was added at a 1:20 ratio. An ultrasonicate bath sonicator operator (SM-100-US, Samarth Electronics, India) dispersed the filler in the ethanol until a uniform dispersion stage was reached. Next, the nanofluid was mixed with PLA granules using a hotplate operator (1-MLH, Remi Elektrotechnik Ltd., India) for uniform dispersion. After completely evaporating the ethanol, the composite was placed in a vacuum oven (GR-58, Nano Tec, India) for a whole day to remove moisture. After twenty-four hours, the composite mixture was collected to prepare the tensile and flexural samples. The mixture was then fed into the injection molding machine (semiautomated horizontal, Deesha Impex Pvt. Ltd, India) as per ASTM Standards.

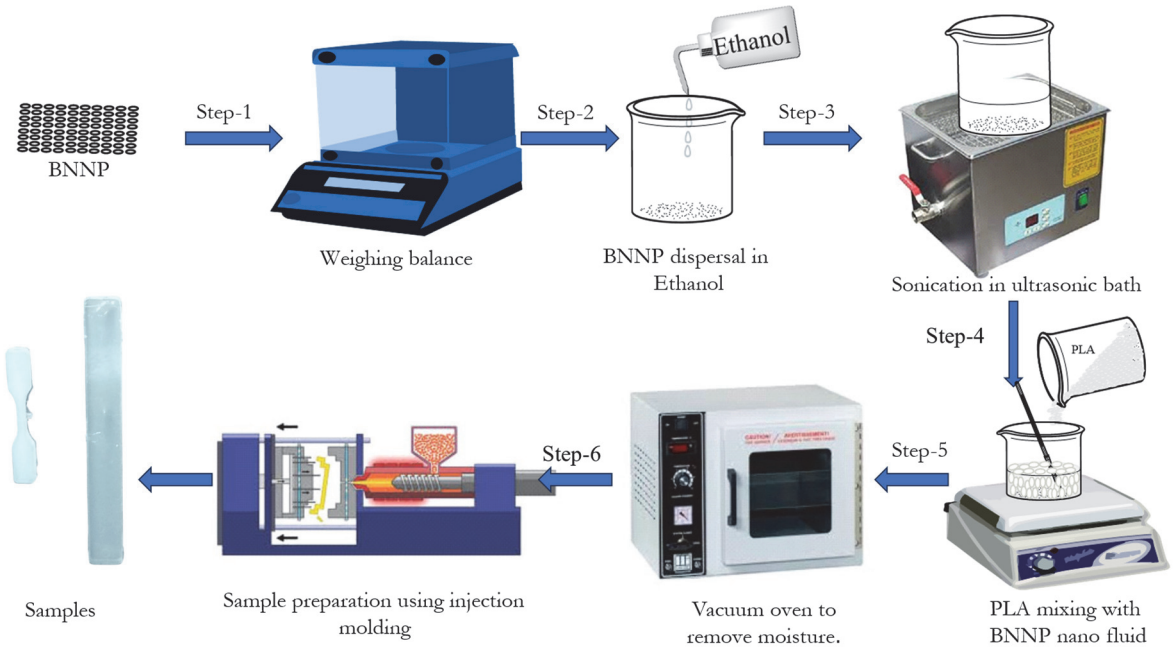

Figure 2: Fabrication steps.

Tensile testing and flexural testing:

A Universal Testing Machine (UTM) (H10KL, Tinius Olsen India Pvt. Ltd., India) was used for the tensile tests as per ASTM D638. The samples were uniformly loaded at a 2 mm/min strain rate under typical atmospheric circumstances. Similarly, flexural testing was carried out by ASTM D790 using the same UTM equipment. The flexural test was performed under atmospheric circumstances and at a 2 mm/min flexural strain rate. All samples underwent five tests, and the average value was noted.

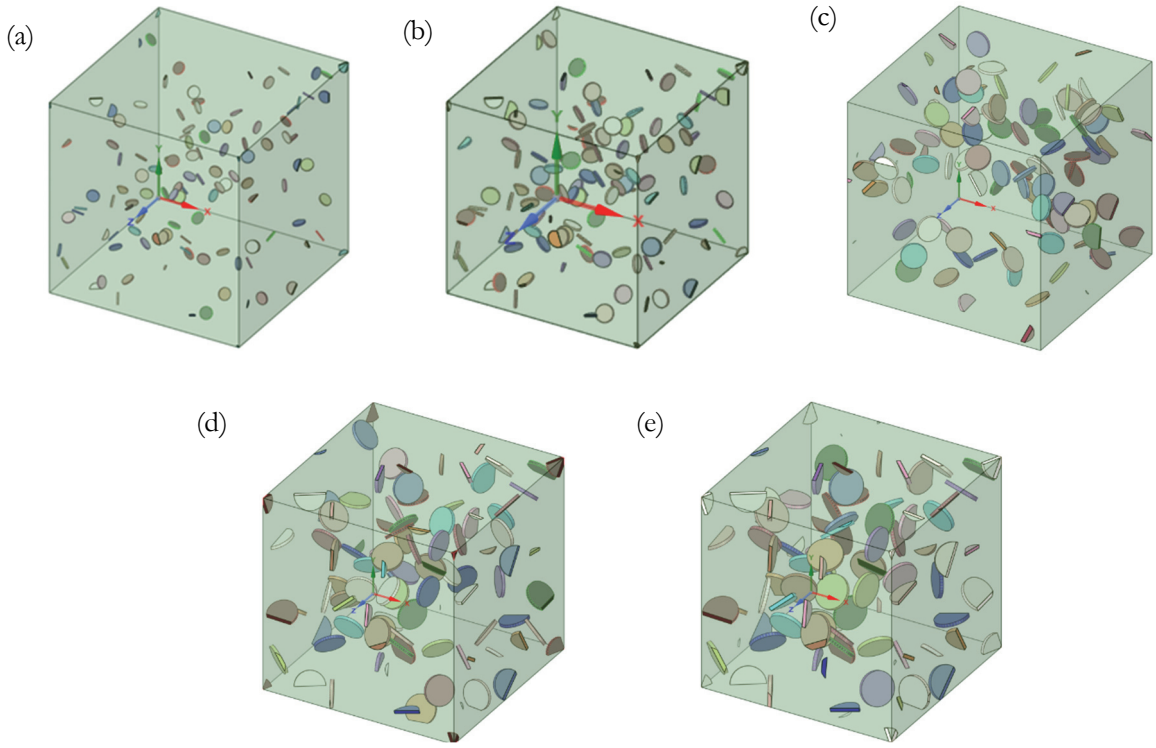

Figure 3: 3D RVE of: a) 0.005 PLA/BNNP, b) 0.01 PLA/BNNP, c) 0.02 PLA/BNNP, d) 0.03 PLA/BNNP, and e) 0.04 PLA/BNNP

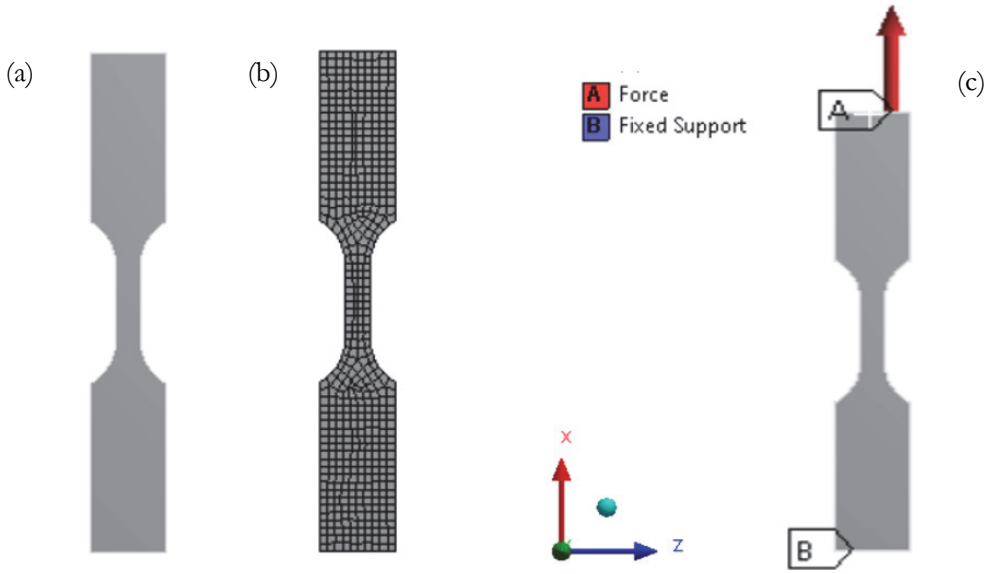

Figure 4: a) Tensile sample, (b) Meshed view (c) boundary conditions.

RVE modelling and fem specifics

Employing the material design module from the ANSYS-2019 workbench, cubic Representative Volume Elements (RVE) were developed in a 1 x 1 x 1 micrometer size. The RVE structures were simulated to calculate the elastic modulus of composite materials by varying the weight % of BNNP i.e. 0.005, 0.01, 0.02, 0.03 and 0.04 PLA/BNNP composite samples, as shown in Figs. 3a to 3e. Convergent analysis was used to determine the RVE dimensions. The material properties computed from the RVE analysis were used for further analysis in the Ansys workbench module, and static structural analysis was carried out for tensile and flexural tests. According to ASTM D638, the tensile geometry is imported into the static structural module, where it is meshed under a quad mesh with 2136 elements and 11247 nodes, as shown in Figs. 4a-b. The bottom faces were constrained, while the load was applied to the top face in the positive x-direction, as illustrated in Fig. 4c. The load value used in the simulation corresponded to the ultimate load from the experimental results. Similarly,

flexural tests were performed in the Ansys static structural simulation environment. The flexural test geometry was modelled following ASTM D790 and meshed with quad elements of roughly 28808 elements and 125609 nodes, as shown in Figs. 5a-b. In this test, the bottom two cylinders are fixed and the top cylinder is loaded in the positive Z direction, with an ultimate load value obtained from the experimental results of a flexural test, as shown in Fig. 5c.

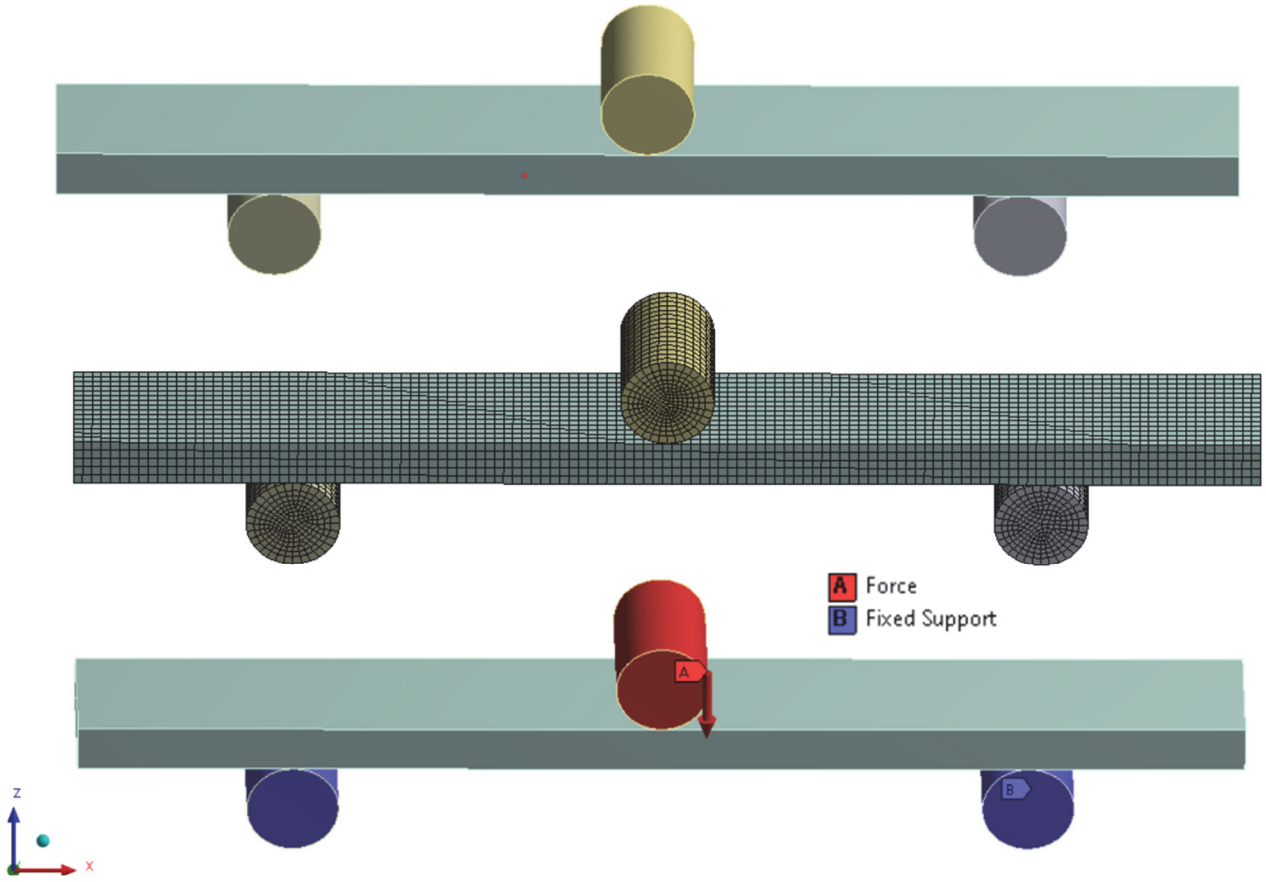

Figure 5: a) Flexural Sample, (b) Meshed View (c) Boundary Conditions with co-ordinate systems.

RESULTS AND DISCUSSIONS

Tensile tests

The stress-strain curve of polylactic acid (PLA) and the different PLA/BNNP composite samples are shown in Fig.6a. The X-axis represents strain (%), and the Y-axis is stress (MPa). Figer.6b. we illustrate the calculation of Young's modulus of PLA and the PLA/BNNP nanocomposites from the stress-strain curve. According to the experimental findings, the pure PLA had an elastic modulus of 3086 MPa and by adding BNNP nanofillers i.e. the 0.005, 0.01, 0.02, 0.03 and 0.04 samples, the moduli rose by 3 %, 6.3 %, 12.28%, 14.62%, and 17.43%, respectively. The ultimate tensile strengths of PLA and the PLA/BNNP composites are displayed in Fig. 6c. The experimentally obtained tensile strength of pure PLA was 20.8 MPa. For 0.005, 0.01, 0.02, 0.03, and 0.04 PLA/BNNP concentrations, the tensile strengths increased by 7%, 11%, 20%, 21%, and 40%, respectively. This enhancement was attributed to the reinforcement of the high Young's modulus of BNNP, which is 0.865 TPa [21], into the PLA matrix leading to load transfer and overall mechanical performance. Additionally, the uniform dispersion of BNNP in the PLA matrix and the strong filler-matrix interaction likely contributed to the increase in composite properties [22, 23]. The tensile test fracture samples were examined using a *ZEISS EVO 10 High-Resolution SEM* (Carl Zeiss AG, Germany) for pure PLA and the 0.04 wt.% PLA/BNNP composite. Fig. 7a shows the fractographic representation of unadulterated polylactic acid (PLA) exhibits a predominantly smooth surface interspersed with particulate matter and residual debris. This suggests plastic deformation occurs before material failure, indicating that the material undergoes some ductile deformation, which improves its capacity to achieve superior interfacial bonding with reinforcement constituents. [24]. In contrast, the fractography of the 0.04 wt.% PLA/BNNP composite, in Fig. 7b, shows

large ridges, which are characteristic of brittle behaviour [25, 26]. These ridges indicate energy absorption and help the material to become stiffer.

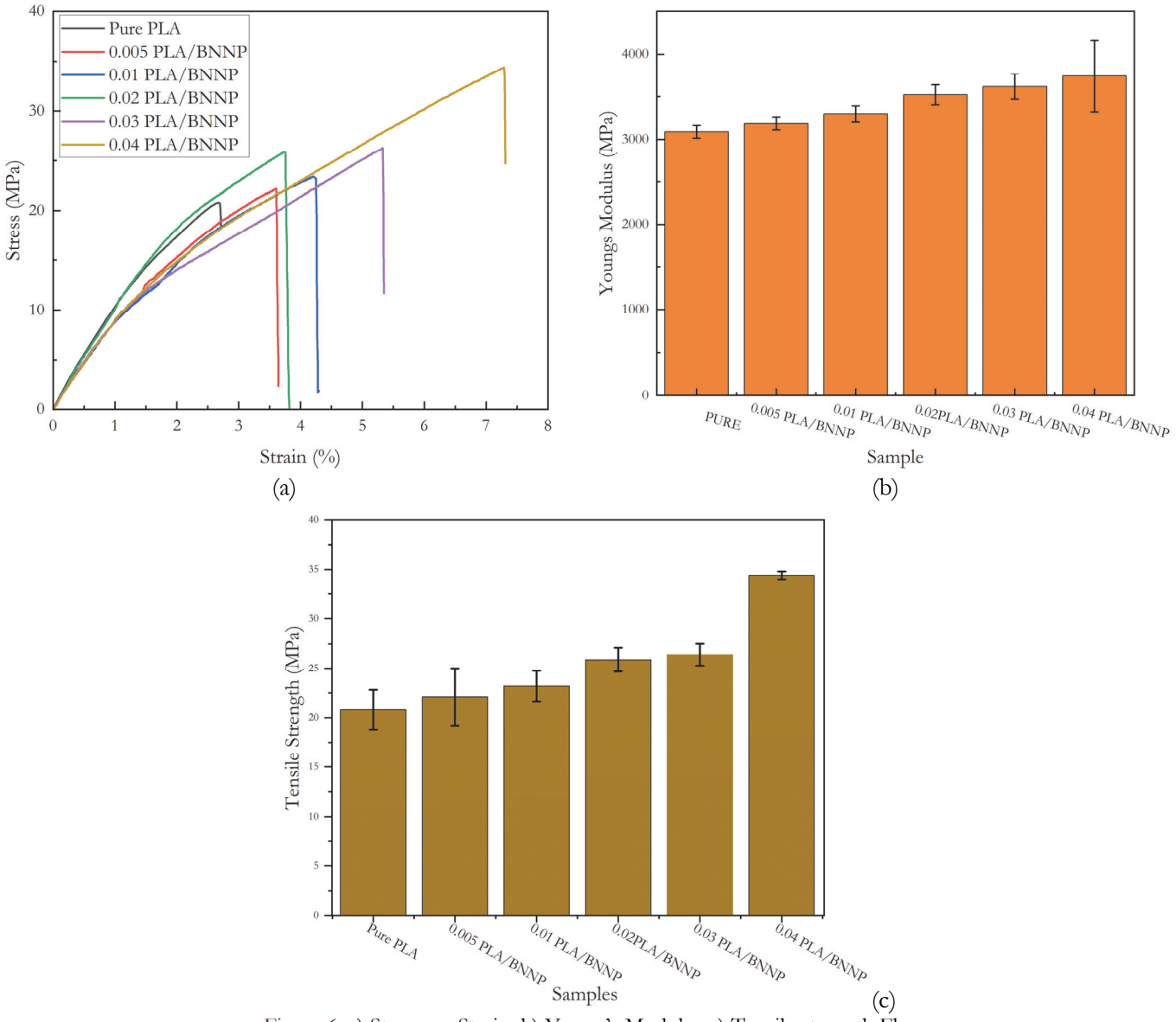

Figure 6: a) Stress vs. Strain, b) Young's Modulus c) Tensile strength Fh.

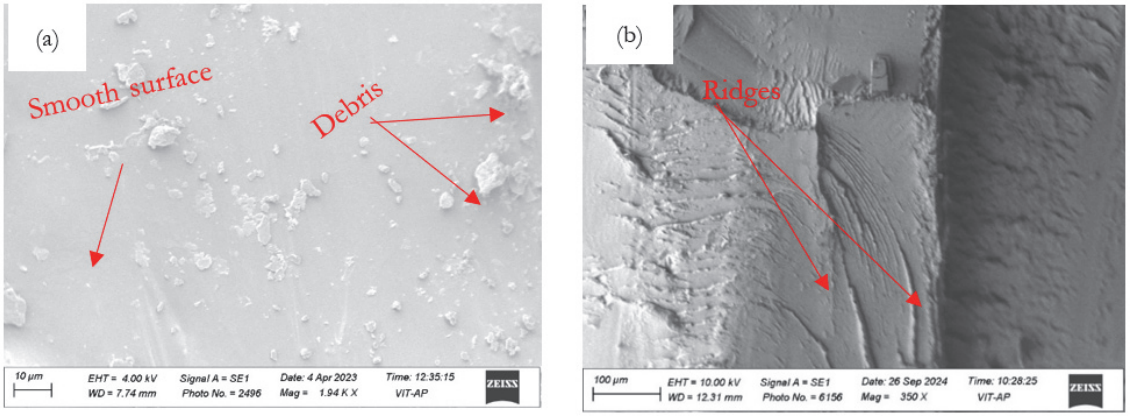

Figure 7: Fractography of a) PLA, b) 0.04 wt.% PLA/BNNP composite.

Flexural tests

Fig. 8a shows the stress-strain relationship between PLA and PLA/BNNP composite samples during the flexural test. The result shows a linear relationship between stress and strain. The flexural strength corresponds to the maximum stress value of the stress-strain graph and is represented in Fig 8b. The pure PLA has a flexural strength of 20.5 MPa, a progressive increase in flexural strength of 12%, 24%, 32%, 51%, and 61% for 0.005 w%, 0.01 w%, 0.02 w%, 0.03 w%, and 0.04 w% respectively was noted for the PLA/BNNP composite samples. The increase in flexural strength with an increase in filler concentration is due to the enhanced stiffness value of the composites [27, 28, 29].

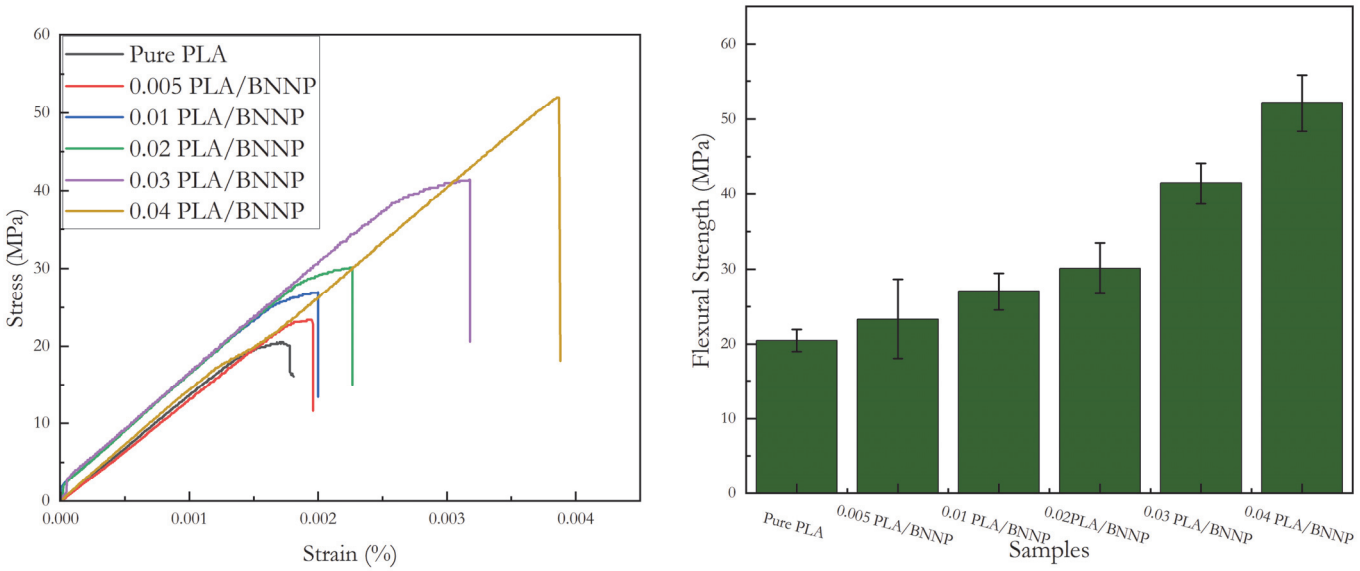

(a) (b)

Figure 8: a) Stress vs. strain, (b) Flexural strength.

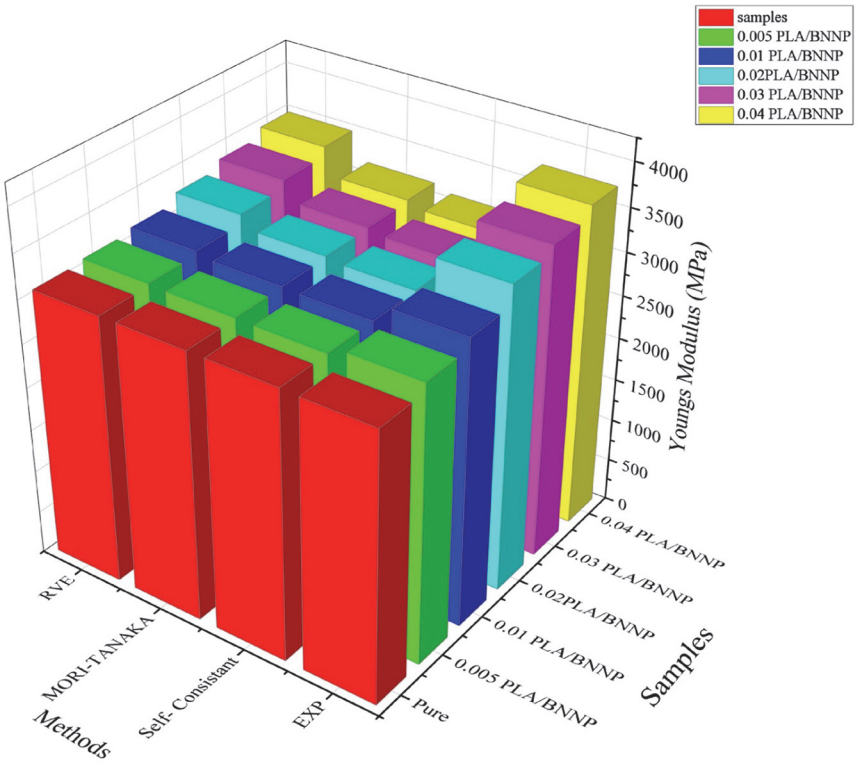

Fig.9 Young's Modulus (MPa) vs Methods for PLA/BNNP composites at various concentrations.

Young's modulus value comparison

This section demonstrates the values of Young's modulus obtained experimentally. It compares them with the predictions from Representative Volume Element (RVE) analysis and micromechanical models, as shown in Fig.9. The experimental Young's modulus for 0.005 PLA/BNNP composite was 3187 MPa, with a deviation of 2%, 2.5%, and 2% for the Self-Consistent, Mori-Tanaka, and RVE approaches, respectively. Similarly, for the 0.01 wt. % PLA/BNNP composite, the variations compared to the experimentally measured Young's moduli were 4%, 5.4%, and 4%. The 0.02 wt. %, 0.03 wt. %, and 0.04 wt. % compositions followed a similar trend, demonstrating that the RVE model effectively aligns with experimentally obtained Young's modulus, with the deviations consistently below 10%.

The agreement confirms the accuracy and predictive capacity of Young modulus between micromechanical predictions and evaluations from the experimental for PLA/BNNP composites. The Mori-Tanaka and Self-Consistent models account for matrix-filler interactions, leading to theoretical predictions and empirical data are closely related. additionally, the Representative Volume Element (RVE) implemented in Ansys simulates the composite microstructural properties by randomly dispersed BNNP fillers within a 1 × 1 × 1 μm^3 cubic domain. This combined technique enhances the accuracy of numerical simulation, adding the predictive potential of micromechanical modeling's for PLA/BNNP composites [30].

FINITE ELEMENT ANALYSIS

Tensile tests

Finite Element Analysis (FEA) was conducted using ANSYS to simulate the tensile behavior of both the pure PLA and PLA/BNNP composites. The stress contour maps, shown in Figs. 10a-f, display the distribution of stress throughout the specimen, with the stress gradually increasing from the wider ends towards the narrow center, which is the most likely location for failure initiation. For pure PLA, the maximum stress value was 23.384 MPa. The PLA/BNNP composite samples with 0.005 wt.%, 0.01 wt.%, 0.02 wt.%, 0.03 wt.%, and 0.04 wt.% BNNP, the stress values increased by 3.7%, 10.7%, 19.8%, 20.7%, and 37.87%, respectively. Fig. 11, Show the comparison between the experimental tensile strength and simulation results. The errors between the simulation and experimental results for pure PLA and the PLA/BNNP composites with different loadings (0.005 to 0.04 wt.%) were 0.495, 0.947, 1.237, 1.975, 1.895 and 2.622 (2.1%, 2.3%, 4.7%, 6.7%, 6.4%, and 6.9%,) respectively. These results show that the simulation and experimental errors were all below 10%, demonstrating the accuracy and reliability of the simulation in predicting the tensile behavior of the PLA/BNNP composites.

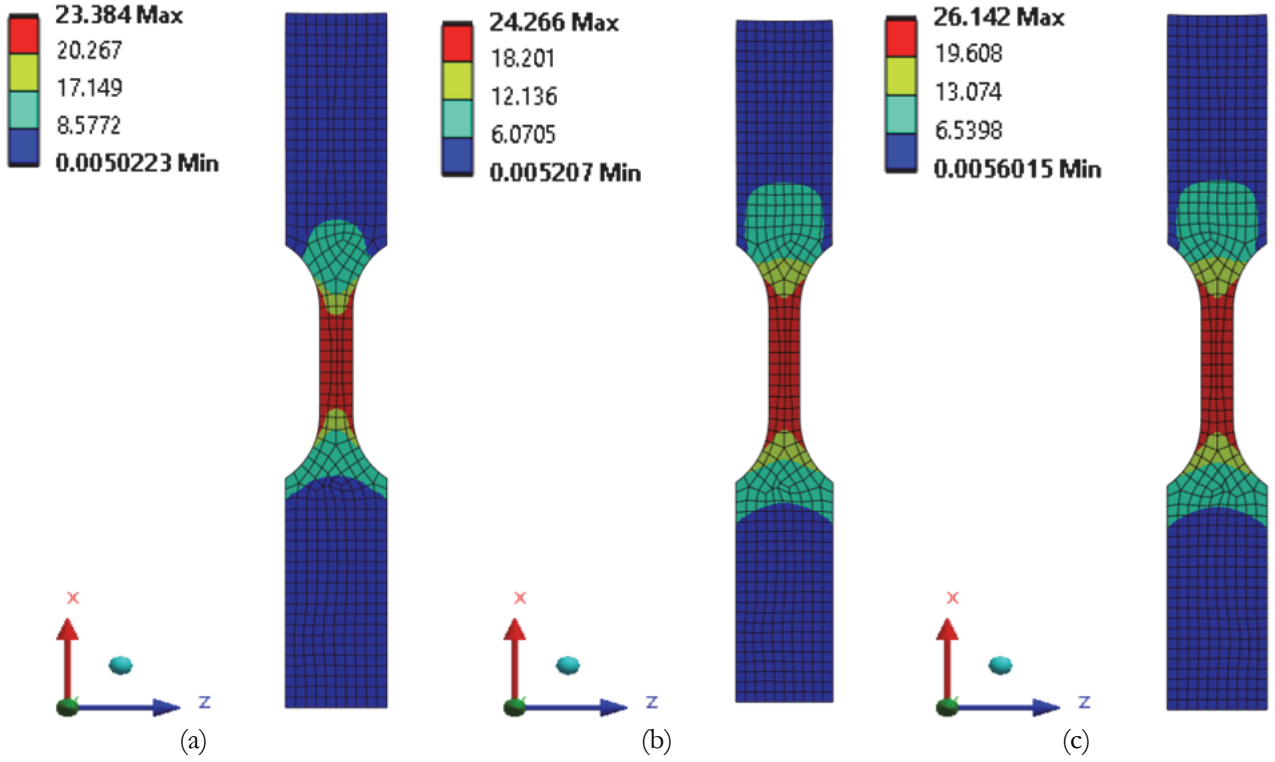

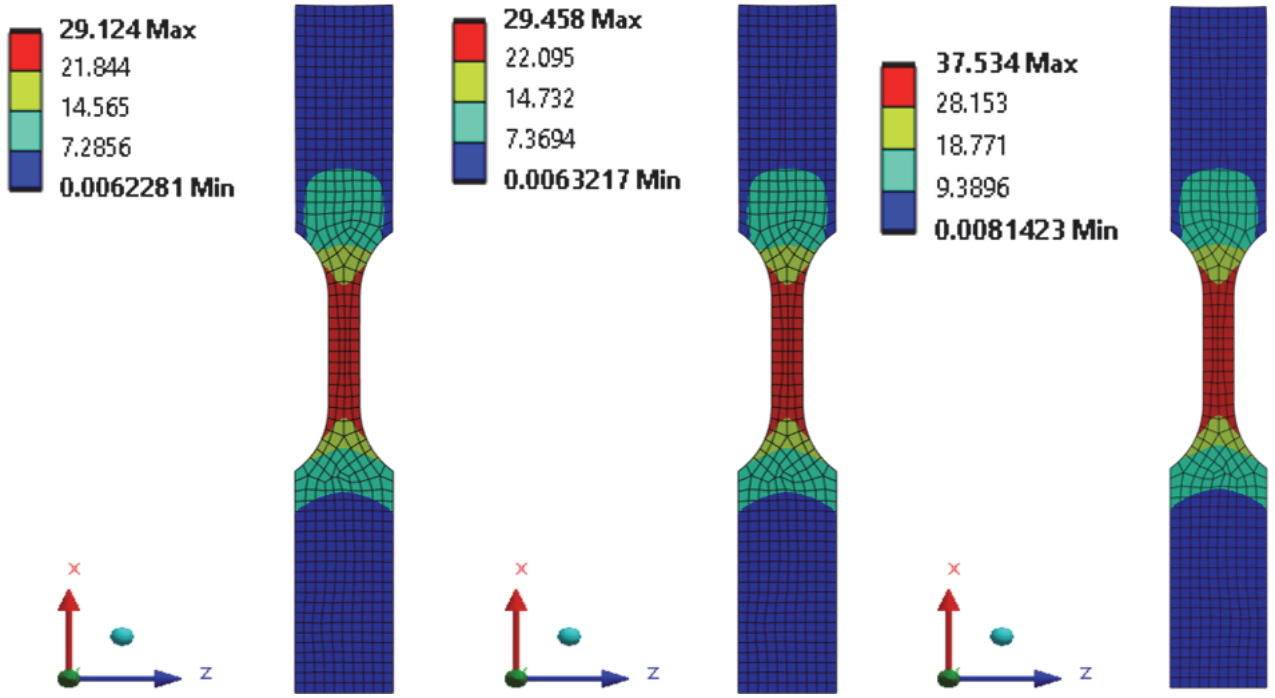

Figure 10: Stress distribution of a) PLA; b) 0.005 PLA/BNNP; c) 0.01 PLA/BNNP; d) 0.02 PLA/BNNP; e) 0.03 PLA/BNNP; f) 0.04 PLA/BNNP tensile sample.

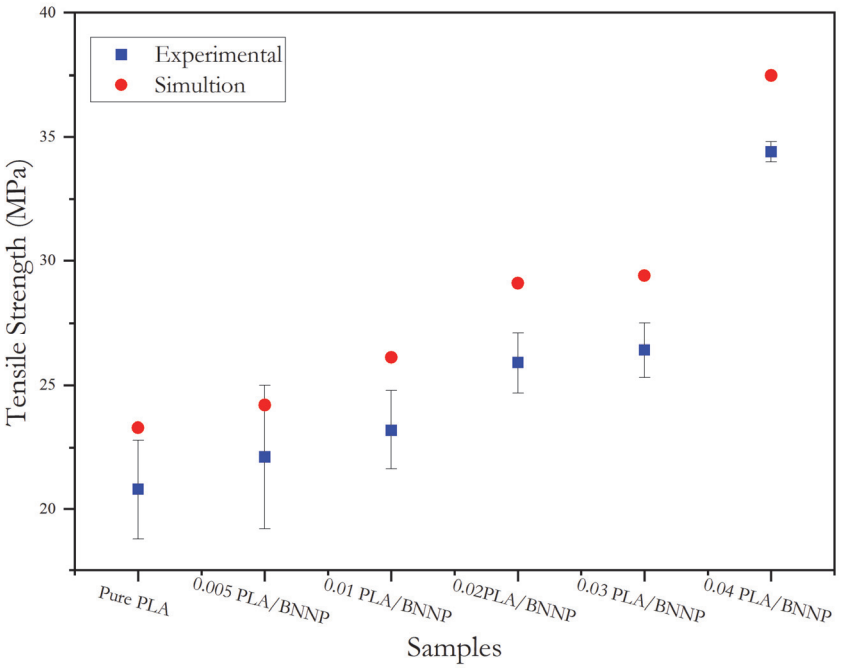

Figure 11: Experimental vs. simulation of tensile strength.

Flexural tests

The Figs. 12a-f illustrates the results of the flexural simulation tests. The stress contour maps demonstrate that the stress is distributed throughout the specimen, with the maximum concentration occurring at the loading point. The pure polylactic acid (PLA) sample exhibited a maximum flexural strength of 20.5 MPa, which is relatively low. However, as we introduced BNNP into the PLA matrix, the flexural strength improved significantly. Specifically, for the PLA composites with 0.005 wt.%, 0.01 wt.%, 0.02 wt.%, 0.03 wt.%, and 0.04 wt.% BNNP, the strength values increased by 21.76%, 23.77%, 33.34%,

49.35% and 59.72%respectively. Additionally, the simulation results were compared with the experimentally determined flexural strengths, as shown in Fig. 13. It revealed a minimal discrepancy, between the simulation and experimental results for the different samples were found to be 1.54, 0.892, 0802, 1.097, 1.308 and 1.376 MPa (6.6%, 3%, 2.6%, 3.2%, 2.8%, and 2.4%). These results indicate a high degree of accuracy in the flexural characterization provided by the simulation, as the errors remained well below 10%. Overall, incorporating BNNP as nanofillers has proved effective in enhancing the mechanical properties of polylactic acid.

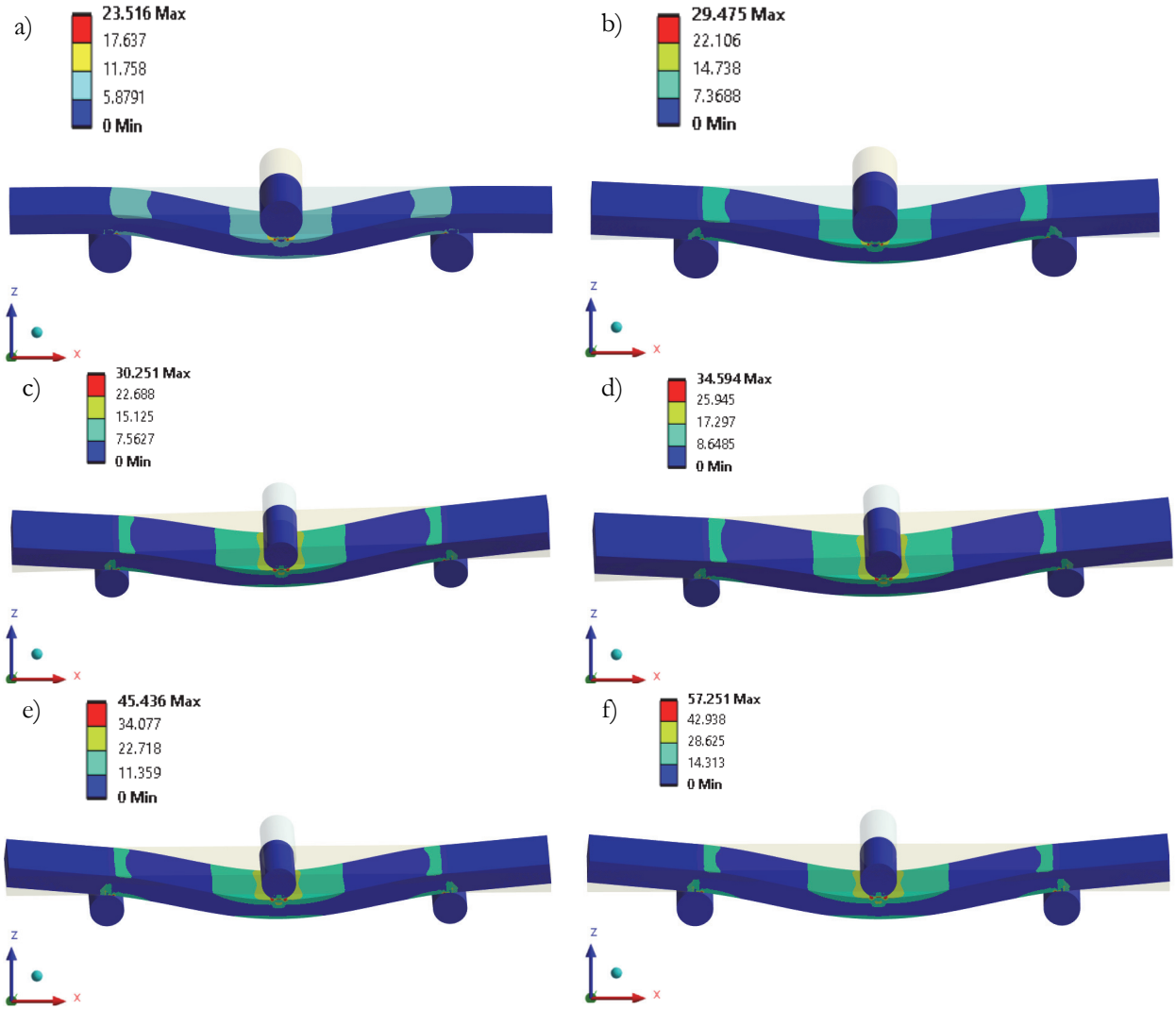

Figure 12: Stresses distribution of a) PLA; b) 0.005 PLA/BNNP; c) 0.01 PLA/BNNP; d) 0.02 PLA/BNNP; e) 0.03 PLA/BNNP; f) 0.04 PLA/BNNP.

CONCLUSIONS

The research described in this paper, fabrication of polylactic acid (PLA) composites incorporated with (0.005, 0.01, 0.02, 0.03 and 0.04) wt.% of Boron Nitride nano-particles (BNNP), and evaluating their tensile and flexural properties using the experimental and Finite elemental methods. The key findings are-

- PLA reinforced with 0.04 weight percent of BNNP shows a significant enhancement of 17.4% Young's modulus, 40% tensile strength, and 61% flexural strength variation compared with pure PLA.
- The Young's modulus predicted by the proposed RVE modeling was near to the experimental results and that of other established micromechanical models.

- The results from the Finite Element Analysis (FEA) were within a 10% error margin compared to experimentally determined tensile and flexural strengths, which demonstrates the effectiveness of the FEA method.

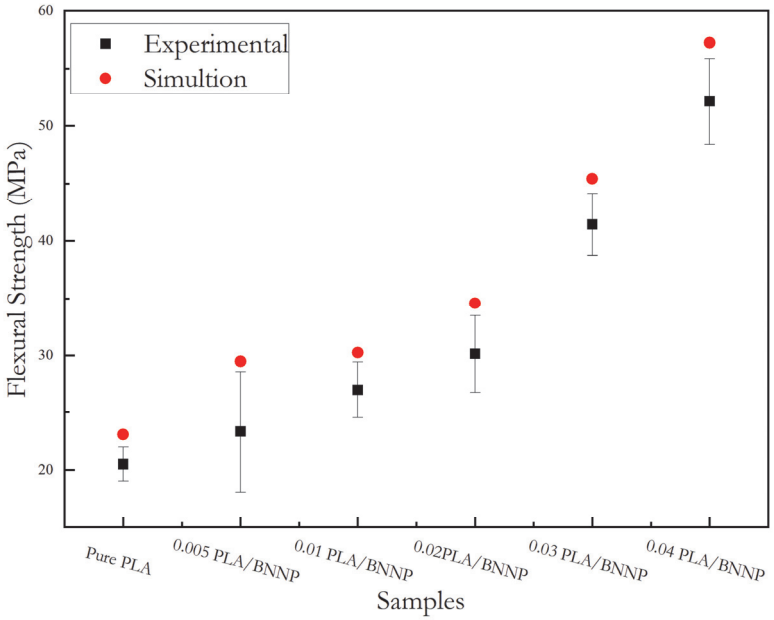

Figure 13: Experimental vs. simulation of flexural strength.

ACKNOWLEDGEMENTS

The authors acknowledge the funding supported by VIT-AP University through the project VIT-AP/SPORIC/RGEMS/2022-23/025. Additionally, the authors thank Mr. E Krishna Murty (Technical Assistant, VIT, Amaravati) and Mr. Loya Prasad (Technical Assistant, VIT, Amaravati) for their support during the sample preparation and testing process.

REFERENCES

[1] Balla, E., Daniilidis, V., Karlioti, G., Kalamas, T., Stefanidou, M., Bikiaris, N. D., Vlachopoulos, A., Koumentakou, I., and Bikiaris, D. N. (2021). Poly(Lactic Acid): A Versatile Biobased Polymer for the Future with Multifunctional Properties—From Monomer Synthesis, Polymerization Techniques and Molecular Weight Increase to PLA Applications, Polymers, 13(11), p. 1822. DOI: 10.3390/polym13111822.

[2] Ajaj, Y., AL-Salman, H. N. K., Hussein, A. M., Khaleel Jamee, M., Abdullaev, S., Omran, A. A., Morad Karim, M., Abdulwahid, A. S., Mahmoud, Z. H., and Kianfar, E. (2024). Effect and Investigating of Graphene Nanoparticles on Mechanical, Physical Properties of Polylactic Acid Polymer, Case Studies in Chemical and Environmental Engineering, **9**, p. 100612. DOI: 10.1016/j.cscee.2024.100612.

[3] Nethula, A., Koka, N. S. S., Chanamala, R., and Putta, N. R. (2023). Experimental Investigations on Preparation of Silica Coated TiO_2 Nanoparticles (S-TiO_2) and Its Mechanical Characterizations as Reinforcement in Polylactic Acid (PLA)/Thermoplastic Polyurethane (TPU) Composites, Eng. Res. Express, **5**(3), p. 035005. DOI: 10.1088/2631-8695/ace2ad.

[4] Mathanesh Thangarajan, Cheow Keat Yeoh, Pei Leng Teh, Wee Chun Wong, Chong Hui Yew, Kang Zheng Khor, Nor Azura Abdul Rahim, and Chun Hong Voon (2024). Dielectric And Mechanical Properties Of PLA-Carbon Composites," IJNeaM, **17**(2), pp. 292–299. DOI: 10.58915/ijneam.v17i2.720.

[5] Petousis, M., Moutsopoulou, A., Korlos, A., Papadakis, V., Mountakis, N., Tsikritzis, D., Ntintakis, I., and Vidakis, N. (2023). The Effect of Nano Zirconium Dioxide (ZrO2)-Optimized Content in Polyamide 12 (PA12) and Polylactic Acid (PLA) Matrices on Their Thermomechanical Response in 3D Printing, Nanomaterials, 13(13), p. 1906.

DOI: 10.3390/nano13131906.
[6] Li, N., Wang, M., Luo, H., Tse, S. D., Gao, Y., Zhu, Z., Guo, H., He, L., Zhu, C., Yin, K., Sun, L., Guo, J., and Hong, H. (2025). Processing and Properties of Graphene-Reinforced Polylactic Acid Nanocomposites for Bioelectronic and Tissue Regenerative Functions, Biomaterials Advances, **167**, p. 214113. DOI: 10.1016/j.bioadv.2024.214113.
[7] Makri, S. P., Xanthopoulou, E., Klonos, P. A., Grigoropoulos, A., Kyritsis, A., Tsachouridis, K., Anastasiou, A., Deligkiozi, I., Nikolaidis, N., and Bikiaris, D. N., 2022, "Effect of Micro- and Nano-Lignin on the Thermal, Mechanical, and Antioxidant Properties of Biobased PLA–Lignin Composite Films," Polymers, 14(23), p. 5274. DOI: 10.3390/polym14235274.
[8] Huang, A., Song, X., Liu, F., Wang, H., Geng, L., Chen, B., Peng, X., Wang, Z., and Tian, G. (2022). Facile Preparation of Anisotropic PLA / CNT Nanocomposites by Hot and Cold Rolling Processes for Improving Mechanical and Conductive Properties, J of Applied Polymer Sci, 139(33), p. e52789. DOI: 10.1002/app.52789.
[9] Solechan, S., Suprihanto, A., Widyanto, S. A., Triyono, J., Fitriyana, D. F., Siregar, J. P., and Cionita, T. (2023). Characterization of PLA/PCL/Nano-Hydroxyapatite (nHA) Biocomposites Prepared via Cold Isostatic Pressing, Polymers, 15(3), p. 559. DOI: 10.3390/polym15030559.
[10] Khammassi, S., Tarfaoui, M., Škrlová, K., Měřínská, D., Plachá, D., and Erchiqui, F. (2022). Poly(Lactic Acid) (PLA)-Based Nanocomposites: Impact of Vermiculite, Silver, and Graphene Oxide on Thermal Stability, Isothermal Crystallization, and Local Mechanical Behavior, J. Compos. Sci., 6(4), p. 112.DOI: 10.3390/jcs6040112.
[11] Vidakis, N., Moutsopoulou, A., Petousis, M., Michailidis, N., Charou, C., Mountakis, N., Argyros, A., Papadakis, V., and Dimitriou, E. (2023). Medical-Grade PLA Nanocomposites with Optimized Tungsten Carbide Nanofiller Content in MEX Additive Manufacturing: A Rheological, Morphological, and Thermomechanical Evaluation, Polymers, 15(19), p. 3883. DOI: 10.3390/polym15193883.
[12] Dileep, K., Srinath, A., Banapurmath, N. R., Umarfarooq, M. A., and Sajjan, A. M. (2023). Mechanical and Fracture Characterization of Epoxy/PLA/Graphene/SiO2 Composites, Frattura ed Integrità Strutturale, 17(64), pp. 229–239. DOI: 10.3221/IGF-ESIS.64.
[13] Daneshpayeh, S., Ashenai Ghasemi, F., and Ghasemi, I., (2022). Experimental Investigation on Mechanical Properties of Nanocomposites Based on Poly Lactic Acid/ Polyolefin Elastomer Reinforced with Multi-Walled Carbon Nanotubes, and Graphene Nanoplatelets, Polymers and Polymer Composites, 30, p. 09673911211060943. DOI: 10.1177/09673911211060943.
[14] Segun, A., Adewuyi, B. O., Ojo, D. O., and Gideon, O. N., (2021). Mechanical and Structural Properties of Nanocarbon Particles Reinforced in Plasticised Polylactic Acid for High Strength Application, JPS, 32(2), pp. 41–56. DOI: 10.21315/jps2021.32.2.4.
[15] Sairy, N. A., Mazlan, N., Ishak, M. R., and Zulkepli, N. N. (2020). Investigation on the Flexural Properties of Nanofillers Loading on the Jute/Carbon/PLA Nanocomposites, JMES, 14(4), pp. 7424–7433. DOI: 10.15282/jmes.14.4.2020.11.0585.
[16] He, H., Pang, Y., Duan, Z., Luo, N., and Wang, Z. (2019). The Strengthening and Toughening of Biodegradable Poly (Lactic Acid) Using the SiO2-PBA Core–Shell Nanoparticle, Materials, 12(16), p. 2510. DOI: 10.3390/ma12162510
[17] Park, I. H., Lee, J. Y., Ahn, S. J., and Choi, H. J. (2020). Melt Rheology and Mechanical Characteristics of Poly(Lactic Acid)/Alkylated Graphene Oxide Nanocomposites, Polymers, 12(10), p. 2402. DOI: 10.3390/polym12102402.
[18] Campuzano, A. J. B., Rezende, R. B., Taborda, N. C., Dos Santos, J. C., Pereira, F. V., and Panzera, T. H. (2024). Physical and Mechanical Properties of Fused Deposition Modelling PLA/Carbon Dot Nanocomposites, Materials Today Communications, 40, p. 110025. DOI: 10.1016/j.mtcomm.2024.110025.
[19] Zhao, S., Zhao, Z., Yang, Z., Ke, L., Kitipornchai, S., and Yang, J. (2020). Functionally Graded Graphene Reinforced Composite Structures: A Review, Engineering Structures, 210, p. 110339. DOI: 10.1016/j.engstruct.2020.110339.
[20] Kanaun, S. K., and Levin, V. M. (2008). Self-Consistent Methods for Composites, Springer Netherlands, Dordrecht. DOI: 10.1007/978-1-4020-6664-1.
[21] Zhang, H., Liu, Y., Sun, K., Li, S., Zhou, J., Liu, S., Wei, H., Liu, B., Xie, L., Li, B., and Jiang, J. (2023). Applications and Theory Investigation of Two-Dimensional Boron Nitride Nanomaterials in Energy Catalysis and Storage, EnergyChem, 5(6), p. 100108. DOI: 10.1016/j.enchem.2023.100108.
[22] Sahu, S. K., and Rama Sreekanth, P. S. (2024). Multiscale RVE Modeling for Assessing Effective Elastic Modulus of HDPE Based Polymer Matrix Nanocomposite Reinforced with Nanodiamond, Int J Interact Des Manuf, 18(9), pp. 6371–6380. DOI: 10.1007/s12008-022-01080-z.
[23] Kushwaha, Y. S., Hemanth, N. S., Badgayan, N. D., and Sahu, S. K. (2022). Free Vibration Analysis of PLA Based Auxetic Metamaterial Structural Composite Using Finite Element Analysis, Materials Today: Proceedings, 56, pp. 1063–1067. DOI: 10.1016/j.matpr.2021.09.482.

[24] Du, Z., Zhu, Z., and Wang, Y. (2018). The Degree of Peri-Implant Osteolysis Induced by PEEK, CoCrMo, and HXLPE Wear Particles: A Study Based on a Porous Ti6Al4V Implant in a Rabbit Model, J Orthop Surg Res, 13(1), p. 23. DOI: 10.1186/s13018-018-0736-y.

[25] Tang, K., Zhang, P., Zhao, Y., and Zhong, Z. (2024). Deep Learning-Based Semantic Segmentation for Morphological Fractography, Engineering Fracture Mechanics, 303, p. 110149. DOI: 10.1016/j.engfracmech.2024.110149.

[26] Sahu, S. K., and Sreekanth, P. S. R. (2022). Artificial Neural Network for Prediction of Mechanical Properties of HDPE Based Nanodiamond Nanocomposite, Polymer (Korea), 46(5), pp. 614–620. DOI: 10.7317/pk.2022.46.5.614.

[27] Zhan, Q., and Yin, C., (2024). A Novel Pervious Concrete Improved by Hexagonal Boron Nitride and Basalt Fiber in Mechanical Properties, Permeability, and Micro-Mechanisms, Buildings, 14(3), p. 778. DOI: 10.3390/buildings14030778.

[28] Yesaswi, C. S., Sahu, S. K., and Sreekanth, P. S. R. (2022). Experimental Investigation of Electro-Mechanical Behavior of Silver-Coated Teflon Fabric-Reinforced Nafion Ionic Polymer Metal Composite with Carbon Nanotubes and Graphene Nanoparticles, Polymers, 14(24), p. 5497. DOI: 10.3390/polym14245497.

[29] Barakhtin, B. K., Sedletsky, R., Perevislov, S. N., Bobyr, V., and Zhukov, A. S. (2023). Influence of Filler Concentration on the Mechanical Properties of a Polymer Composite," MSF, 1082, pp. 121–126. DOI: 10.4028/p-4s46s1.

[30] Zyganitidis, I., Arailopoulos, A., and Giagopoulos, D. (2022). Composite Material Elastic Effective Coefficients Optimization by Means of a Micromechanical Mechanical Model, Applied Mechanics, 3(3), pp. 779–798. DOI: 10.3390/applmech3030046.